Nonlinear Mechanics of Two-Dimensional Carbon-Carbon Composite Structures and Materials

Edward L. Stanton* and Thomas E. Kipp†
PDA Engineering, Santa Ana, California

The inelastic mechanics of isotropic materials are usually modeled by scalar functions of the material stress or strain state. Simple effective stress-strain models work well because of the material symmetry and homogeneity usually found in structural materials, and because a single deformation mechanism accounts for inelastic strain behavior. In contrast, laminated carbon-carbon composites are anisotropic with a weak matrix phase and exhibit at least two inelastic deformation mechanisms in coupon tests. The motivation for the present work was the bimodular nonlinear strain response found in testing involute cylinders of a low modulus carbon-carbon material typical of a composite used in nozzle components for several years and now used in several industrial products to replace asbestos. These experimental results raised basic questions about nonlinear material modeling and characterization for this class of composites. The present paper describes results from a program that developed and demonstrated a nonlinear model for two-dimensional carbon-carbon composites based directly on coupon stress-strain data. A low modulus bidirectional material, K-KARB, was used to validate the model in room temperature tests.

Introduction

THE motivation for this study was the bimodular nonlinear response found by Davis in testing involute cylinders of low modulus K-KARB carbon-carbon material.[1] These results raised questions that could not be answered using then available models and data. The purpose of the present effort is to experimentally study and to model nonlinear material and structural behavior in this class of composites. The scope of the experimental effort included a comprehensive test series by Davis at the Aerojet Strategic Propulsion Co. (ASPC)[2] that cannot be described fully herein. The scope of the analysis effort included several nonlinear material models and a finite element model for structural analyses. We were able to show that material frame stress-strain data and a simple interaction formula predict the unusual bimodular response in test cylinders reported earlier as well as our test cone data from the present test series. A mechanism is postulated to explain this behavior, which is in general agreement with subsequent microstress analyses by Jortner.[3] A pseudoforce formulation was used for finite element work based on material frame strains at the optimal strain recovery points in the sense defined by Barlow.[4] The PATCHES-III code was used for structural analyses in order to model fiber orientation in composites of involute construction as described by Pagano.[5] Fibers produce involute spirals in this construction, which complicates structural modeling in that distribution functions are required for three Euler angles to define material geometry in each element.

An important material characterization issue addressed during the program was to determine if fill tension response in coupons is representative of fill fiber response in hoop tension for involute cylinders and cones. The utility of flat panel or coupon data for nonlinear structural analyses is dependent on this issue, and our results show that these data are characteristic of nonlinear involute composites. Even high arc angle cylinders that ultimately failed in interlaminar shear under internal pressure followed the coupon predicted response. Also, we were able to develop the full compressive strength of the warp fibers in an involute test cone. Comparisons between strain gage data and finite element analyses are provided for mechanical load conditions at room temperature.

Nonlinear Behavior in 2D Carbon-Carbon Materials

To model the mechanics of a two-dimensional (2D) carbon-carbon material, it is helpful to first examine the constituents and comment on the scale at which events controlling macroscopic behavior take place. The constituents making up the fibrous phase of K-KARB are warp and fill graphite yarns. Plain-weave graphite cloth has some crimp or waviness in both the warp and fill directions that forms a textured surface in the laminate (see Fig. 1). A detailed treatment of the geometry and structural mechanics of fabrics may be found in Ref. 6. Adjacent plies nest peak-to-valley, creating a mechanical impediment to interlaminar shear and nonuniform microstress fields that largely determine composite strength and nonlinear material behavior which is bimodular. Mechanistic models that predict the bimodular behavior of low modulus composites show[3] this behavior to be opposite to that found in high modulus composites with a strong matrix phase.[7] Coupon data from the ASPC tests[2] suggest that nonlinear fill tension behavior is associated with some form of crossover damage between warp and fill yarns in the K-KARB composite. This damage mechanism, inferred from both warp transverse strain data and fill extensional strain data, allows relative movement between yarns locally. This mechanism affects both fill tensile stiffness and warp-fill shear stiffness. Identification of this damage mechanism and its effect on stiffness was the key to modeling fiber-dominated nonlinear behavior in K-KARB composites. Additional tests to confirm our findings and better characterize the mechanism are suggested. It is possible, for example, that thermal as well as mechanical properties are changed by crossover damage and that the morphology is not simple microcracking.

Presented as Paper 84-0956 at the AIAA/ASME/ASCE/AHS 25th Structures, Structural Dynamics and Materials Conference, Palm Springs, Calif., May 14-16, 1984; received June 18, 1984; revision received Sept. 24, 1984.

*Program Manager. Member AIAA.
†Engineering Associate.

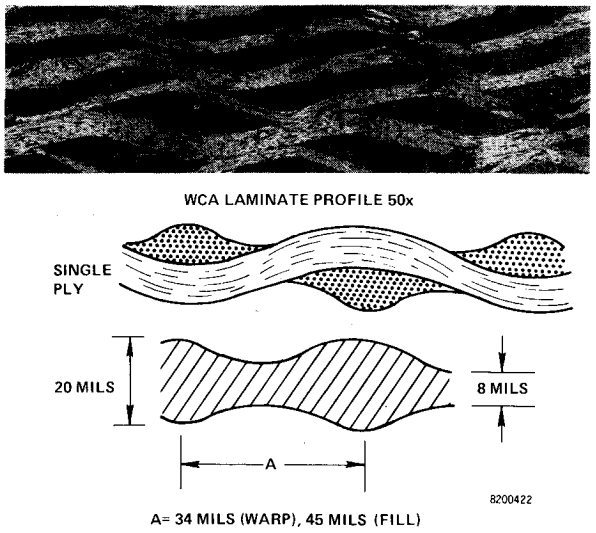

Fig. 1 Plain weave laminate schematic.

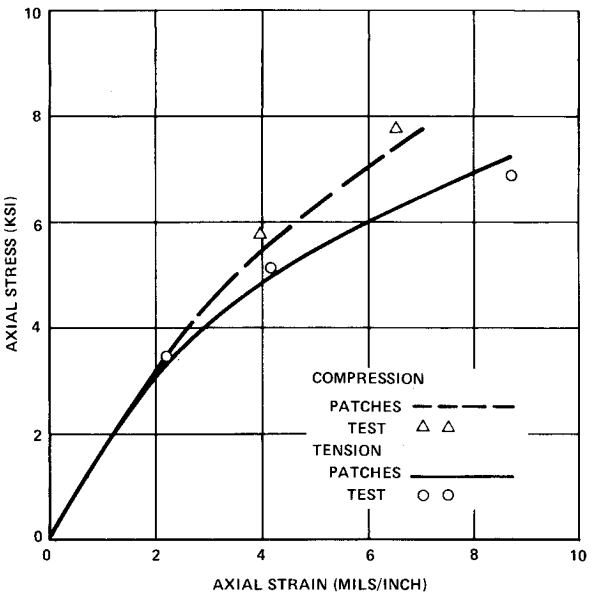

Fig. 2 Involute cylinder bimodular axial response.

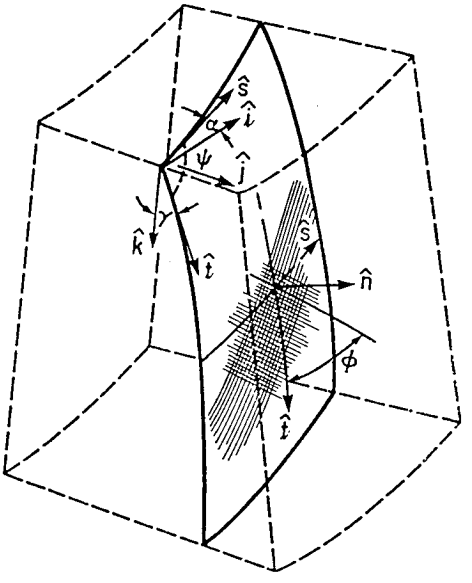

Fig. 3 Involute material geometry model.

Nonlinear Modeling of 2D Carbon-Carbon Materials

Several years ago in careful laboratory tests, Jortner[8] showed evidence of biaxial softening in ATJ-S graphite specimens. Since a single deformation mechanism (microcracking) seemed to be at work, these results led Batdorf[9] and Jones[10] to seek other state variables for nonlinear material modeling and to reject distortional energy formulations. These new models were able to reproduce Jortner's data with good accuracy. However, there are problems in trying to model materials with multiple damage or nonlinear deformation mechanisms with a single state variable such as macrostress-strain potential energy. This situation is entirely analogous to problems described by Owen[11] in modeling glass fabric composite failure surfaces with a single polynomial surface such as the Tsai-Wu. Our own testing shows there are multiple deformation mechanisms active in K-KARB, suggesting that a nonlinear model for this material could require as many parameters as the linear model for macrostress-strain response. It is, of course, possible to formulate nonlinear material models based on microstress in a representative volume of the material. Delneste and Perez[12] used such a model for four-dimensional carbon-carbon with good results. In their model, the fibers respond in a purely linear manner, and this assumption seems to work well for constructions with straight fibers. Woven ply 2D carbon-carbons are very different constructions and the fill fibers respond in a nonlinear manner at low stress levels. To account for both matrix and fiber nonlinear behavior, K-KARB, a model based on material frame strains and coupon test data, was developed.

The nonlinear material model, K-KARB, requires all nine coupon tests normally used for strength to describe nonlinear stress-strain behavior. It is a very simple model that requires comprehensive test data and computer-aided analyses. The key interaction term couples warp-fill shear stiffness to fill tension using a rule-of-mixtures. Other interactions are second order because a weak carbon matrix phase produces small transverse strains. The model was validated by comparison to our cylinder and cone test data and by comparison to several other involute composite tests on other programs.

One important advantage of this approach to modeling 2D carbon-carbons is that tension and compression behavior in the principal material directions and pure shear response are modeled exactly. No single state variable that represented all nonlinear behavior with one or two test curves was found. The presence of multiple inelastic deformation mechanisms in K-KARB made this difficult, if not impossible. In effect, material frame strains are the state variables of the K-KARB model. Multiaxial effects normally represented by a state variable like potential energy or distortional energy are minimal in K-KARB because of the porous matrix phase. A rule-of-mixtures represents the one first-order interaction observed in tests. Although simple, the model proved effective and was able to reproduce the tension-compression differences observed earlier by Davis[1] in biased involute test cylinders, Fig. 2. It also predicted the measured strain response of all the involute cylinders and cones tested on this program.

Finite Element Model

In an earlier work,[13] a parametric cubic finite element was chosen for modeling the material geometry peculiar to the involute construction used in most K-KARB composites. Applications of this element to cylindrical test specimens produced results in good agreement with Pagano's[5] original linear finite difference model for involutes. A feature of this element is the use of tricubic functions for modeling variable material orientation within an element. Three angles, Fig. 3,

define material orientation at each point; arc angle α, helix angle ϕ, and tilt angle γ. They are generated automatically in PATCHES-III based on the startline formulation of Pagano.[14] Material nonlinearity is treated as a pseudoforce term in the equilibrium equations using an analogy between inelastic strains and applied forces introduced by Lin.[15] This reduces the nonlinear problem to successive linear elastic problems with approximate inelastic strains that converge to the actual inelastic strains under fairly general conditions. In this development, we assume the material homogeneous.

Separate the total strain into elastic, thermal, and inelastic components

$$\epsilon = \epsilon^E + \epsilon^T + \epsilon^P$$

and define the mechanical strains as

$$\epsilon^M \equiv \epsilon - \epsilon^T$$

then the pseudo-force term in the matrix displacement equilibrium equations can be written

$$F_p = \int_V [P]^T [B]^T [C] \epsilon^P dV$$

$$= \int_V [P]^T [B]^T [D]^T [C_m] \epsilon_m^P dV$$

$$= \int_V [P]^T [B]^T [D]^T [\Delta C_m] \epsilon_m^M dV$$

where the $[P]$ and $[B]$ matrices for general shapes and axisymmetric shapes are different. The matrices appearing in the definition of F_p and their dimensions are as follows.

ϵ_m^M = mechanical strain vector in the material frame, dimension 6

$[\Delta C_m]$ = difference between the material frame initial stiffness matrix and secant stiffness matrix evaluated at the current strain state, dimension 6×6

$[D]$ = strain transformation matrix from material frame to reference frame, dimension 6×6

$[B]$ = strain-displacement transformation, dimension 6×9

$[P]$ = gradient of the finite element displacement functions required by strain-displacement equations, dimension 192×9 for general shapes and 48×9 for general axisymmetric shapes

F_p = pseudo-force vector for work associated with inelastic strains ϵ^P, dimension 192 for general shapes and 48 for general axisymmetric shapes.

The computational cost of generating the pseudo-force vector is quite small because strains and secant properties are evaluated only at the 27 Barlow points.[16] Once these data are computed for a finite element, the volume integration for the pseudo-force vector is exactly the same as that for a thermal load vector.

Nonlinear Material Model

Unlike monolithic graphite or graphite epoxy, no single inelastic deformation mechanism such as microcracking or matrix shear characterizes all the first-order nonlinear effects observed in K-KARB. As described earlier, there are both fiber and matrix dominated mechanisms active as well as uniaxial tension-compression differences. The two basic modeling approaches normally used are mechanistic models of a representative volume element response and state variable models of the composite stress-strain response. The latter are usually effective stress or effective strain parameters. Our data and the general difficulty in finding a single polynomial failure surface for all combined stress states in fiber-reinforced composites led us to reject these models. Mechanistic models tend to be computationally expensive and still contain empirical factors for carbon-carbon that must be obtained from composite tests. That being the case, we chose to use a model based directly on the coupon stress-strain data. In effect, the material frame strains are the "state" variables of the model.

$$\sigma_i = S_{ij}^{-1}(\epsilon_i)\epsilon_j$$

where

$$S_{11} = 1/E_W^S(\epsilon_W) \quad S_{22} = 1/E_F^S(\epsilon_F) \quad S_{33} = 1/E_N^S(\epsilon_N)$$

$$S_{44} = f_4/G_{WF} \quad S_{55} = 1/G_{WN}^S(\gamma_{WN}) \quad S_{66} = 1/G_{FN}^S(\gamma_{FN})$$

and all off-diagonal S_{ij} are equal to their initial linear elastic values. The subscripts W, F, N refer to the warp, fill, and normal directions which are the material frame coordinate directions.

To account for multiaxial stress interactions, we adopted a very simple interaction formula based on the postulated crossover damage mechanism discussed earlier. The single interaction term in the nonlinear K-KARB model

$$f_4 = \frac{G_{WF}}{(1-X)G_{WF}^S(\gamma_{WF}) + XG_{WF}^T(\gamma_{WF}^0)}$$

where

$$X = \epsilon_F/\epsilon_F^0, \quad \epsilon_F > 0$$

is simply a rule-of-mixtures that degrades the warp-fill shear stiffness to its limiting tangent modulus with increasing fill tension. Nonlinear transverse strain effects are ignored as second order which is similar to the Batdorf model for graphite in tension. Coupon stress-strain data in both tension and compression are required for all six components which are available from characterization tests for uniaxial strength. This is the fundamental difference between the K-KARB model and those normally used for nonlinear materials. Instead of finding a single stress-strain diagram that matches all test data with the aid of some special state variable, all six stress-strain diagrams are used directly. This approach is feasible with computer data bases and computational mechanics, but would be difficult to use with analytical mechanics.

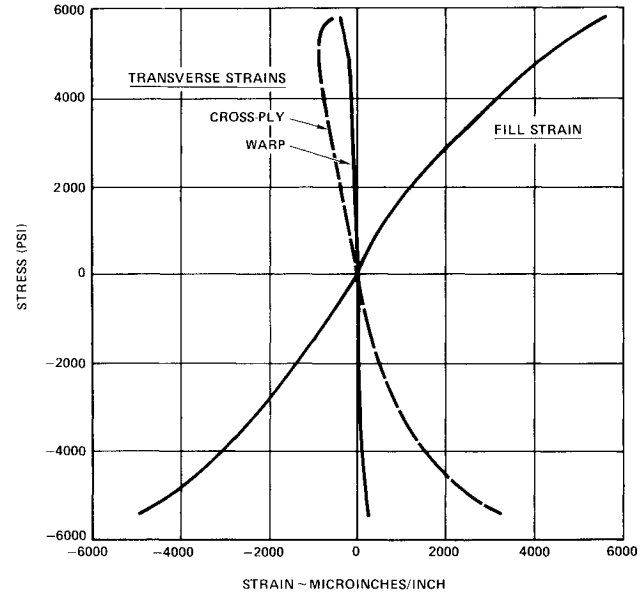

Fig. 4 Fill coupon tension and compression results.

There are a number of features of the K-KARB model that merit comment. First, the assumption of constant off-diagonal S_{ij} preserves the symmetry condition $S_{ij}^t = S_{ij}^c$ observed in the initial tension-compression response of K-KARB coupons. Second, this same assumption forces the Poisson ratios ν_{ij} to change in proportion to the E_{ii} changes and, since they decrease, the ν_{ij} must decrease. This is consistent with the data for tensile fill tests, but not compression. In compression, for instance, Fig. 4, the interlaminar normal strain increases nonlinearly. These second-order effects have not presented any problems in using the model to predict the measured response of involute composites.

The first-order interaction, caused by crossover damage, induces changes in warp-fill shear stiffness. Warp transverse strains from the fill coupon tension test are shown, greatly magnified, Fig. 5, to explain this behavior. The linear initial response corresponds to well-bonded warp-fill fiber crossovers in which the square weave responds without interfiber slip. At about 2400 psi, this bond breaks down and slip between fibers allows the fill fiber to strain with very little increase in warp strain. This behavior continues to about 5000 psi, at which point large increases in warp strain begin. In fact, the rate is the same as the matrix-dominated cross-ply transverse strain curve.

At impossibly high loads, the S_{ij} matrix with fixed off-diagonal terms will fail to be positive definite and this condition is checked whenever an S_{ij} matrix is created. However, the S_{ij} matrix is well conditioned for K-KARB, even for loads near failure. The computer model extends the stress-strain diagram beyond the highest input values using the tangent modulus at that point. This is necessary for computational stability because any off-table strain computed during the iterative solution would appear as a soft or perfectly plastic material point.

Model Validation and Evaluation

Validity of a computational model for nonlinear materials in this paper means that it is self-consistent, satisfies material frame indifference and material stability. The validity of classical models like a deformation theory is, of course, well established; the only issue is the validity of our pseudo-force finite element computational model. Phenomenological models are checked for self-consistency using the model to analyze the very same test specimens used to provide input data for the analysis. Also, the converged secant properties were used in linear analyses and the stress-strain results checked against the nonlinear analyses. After model validation, the performance of a model in terms of convergence characteristics and accuracy in comparison to structural test data can be evaluated.

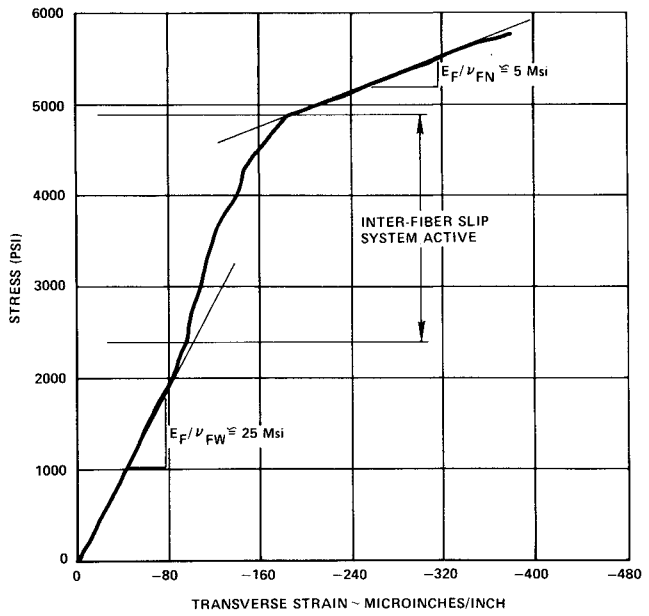

Fig. 5 Fill coupon warp transverse strain results.

Involute Cylinders Test Correlation

There were four involute cylinders built and tested at Aerojet. Three were nominally identical and the fourth, Table 1, had a very high arc angle. All four cylinders, their instrumentation, and test results were uniformly good. Comparison of the $\bar{\alpha} = 10$ deg cylinder strengths under combined load with a polynomial failure envelope based on coupon data in an earlier report[2] confirms the quality of the specimens and testing. Table 2 summarizes the loads and strains just prior to failure and a complete set of data is provided in the test report. Comparison of the hoop strains with analysis was best for the high arc angle cylinder that failed in an interlaminar mode and good for all four cylinders.

The three $\bar{\alpha} = 10$ deg cylinders had axial strain responses that were very nearly linearly to failure. In all cylinders, the hoop strain response was nonlinear and comparisons with the K-KARB model show excellent agreement for tension fields, Fig. 6, and good agreement for tension-compression fields, Fig. 7. Many more tests would be necessary for a statistically significant validation of the K-KARB model for cylinders. All of our applications of the model to cylinders including the earlier 1979 Aerojet test cylinders have compared well with measured strain data.

Involute Cone Test Correlation

Three nominally identical cones were tested to evaluate the K-KARB model in a structural composite. The most significant parameter not studied was temperature, which was beyond the scope of the program. However, this program was unique in that coupon, cylinder, and cone specimens were designed, fabricated, and tested all in support of

Table 1 Aerojet involute test cylinders

Cylinder	$\bar{\alpha}$, deg	ϕ, deg	Axial load, lb/step	Pressure load, psi/step
101-584	10	0	0	20
101-585	10	0	−2000	30
101-586	10	0	1000	20
101-587	15	0	−2000	30

Table 2 Involute cylinder data prior[a] to failure

Cylinder	Axial load, lb	Pressure, psi	Axial strain, μin./in.	Hoop strain, μin./in.
101-584	0	501	−585	2934
101-585	−29965	452	−2530	3300
101-586	34985	701	4468	3692
101-587	−32035	475	−2943	3249

[a]Cylinders failed during next load increment.

Table 3 Involute cone data prior[a] to failure

Cone	Axial load, lb	Pressure, psi	Meridional strain, μin./in.	Hoop strain, μin./in.
101	−46861	0	−3821	314
102	0	290	−622	2879
103	−28660	292	−2962	3120

[a]Cones failed during next load increment.

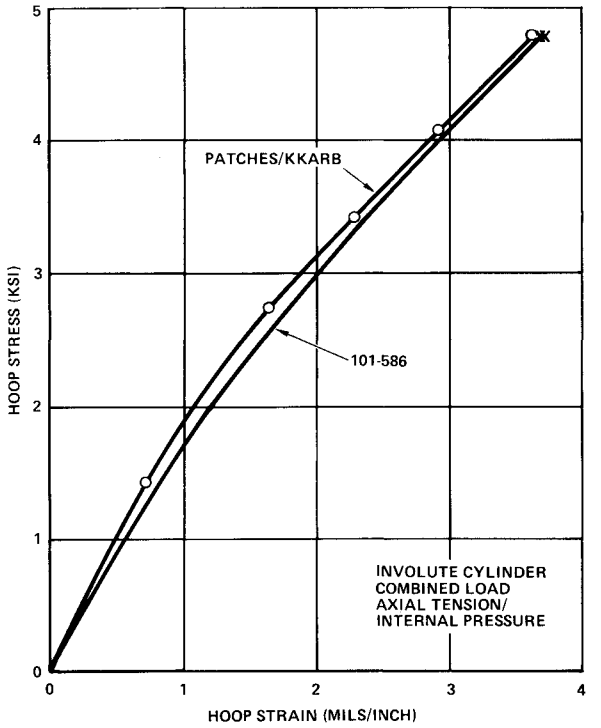

Fig. 6 Test cylinder −586 hoop strain comparisons.

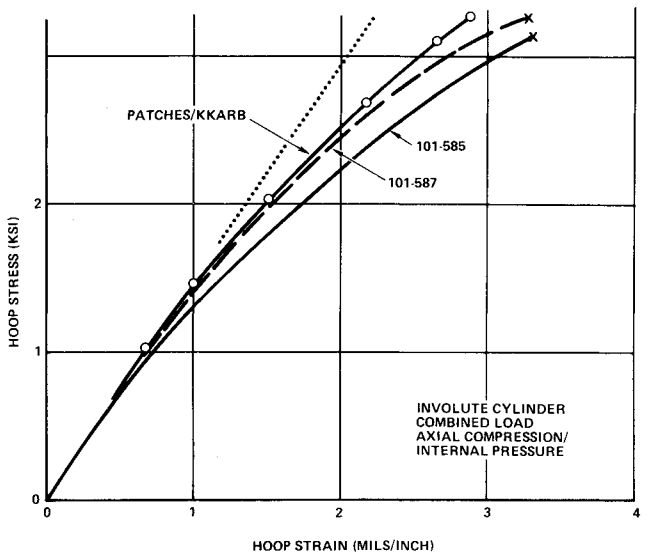

Fig. 7 Test cylinders, −585, −587 hoop strain comparisons.

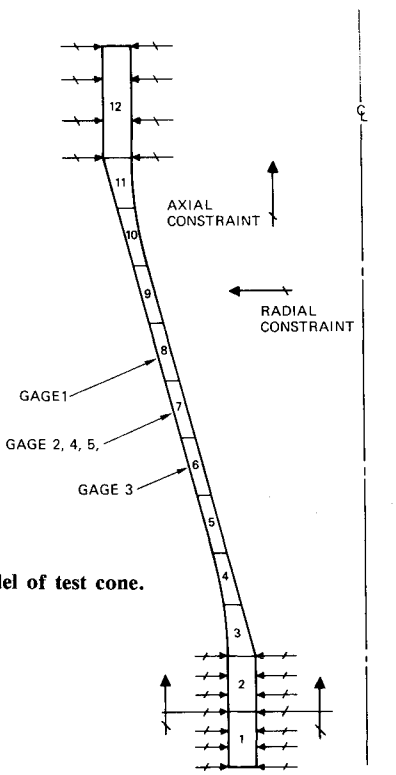

Fig. 8 PATCHES-III model of test cone.

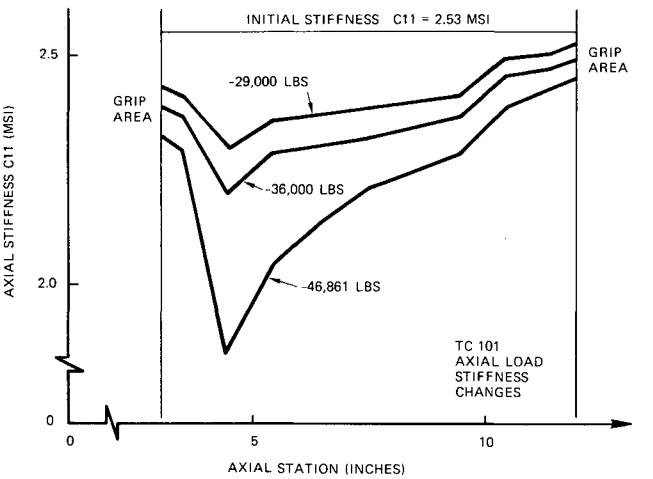

Fig. 9 Test cone 101 warp stiffness changes under load.

developing a nonlinear material model for finite element structural analyses of 2D carbon-carbon composites.

The ideal material geometry is described in the AFRPL report[2] and conditions in the gage section just prior to failure are shown in Table 3. It should be noted that only the combined load test, cone 103, was critical in the gage section. Strain gages were bonded to the outside surface in the hoop and axial directions and along their bisector. In this paper, meridional gages are referred to as axial and they are measuring essentially warp strain in that the helix angle at the cone surface is only 5 degrees.

The PATCHES-III model of the test cone, Fig. 8, used 12 axisymmetric elements with torsion included and with automated involute material geometry modeling and K-KARB modeling of the nonlinear material properties. Axial loads are reacted at the station where the cone is mechanically connected to the grips. This end of the cone is fixed during axial and pressure loading with axial loads applied at the large diameter end through a similar set of grips. This same model with linear properties was used to set test load increments. A complete linear analysis, including model generation, required less than 8 min on the VAX 11/780 and a complete nonlinear solution 17 min.

Test cone 101 was loaded in axial compression to determine if the linear warp compression behavior observed in coupons would describe an involute cone loaded to failure. Response in the gage section was very nearly linear to failure and only the forward gage, gage 3, showed a small amount of inelastic strain. Changes under load of the computed warp secant stiffness down the length of the cone from the PATCHES-III analysis, Fig. 9, indicate a failure site near station 4.5 and that is where failure occurred.

The warp stress, −12,400 psi, at failure was slightly higher than the coupon strength and could reflect a thickness effect. The P/A axial stress at the minimum area station, also 4.5,

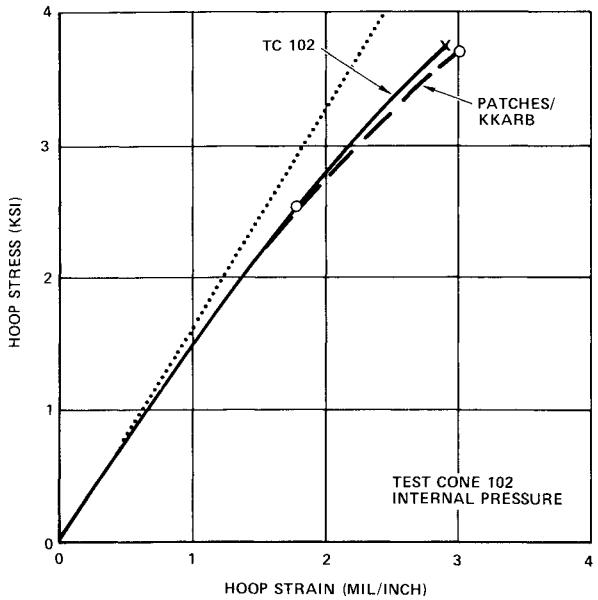

Fig. 10 Test cone 102 hoop strain comparisons.

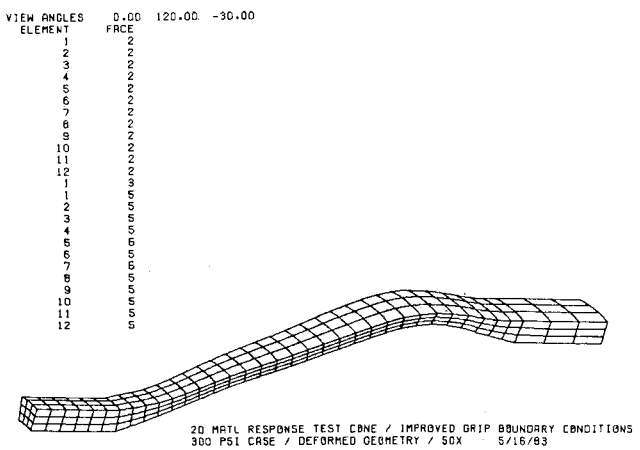

Fig. 11 Test cone 102 deformations.

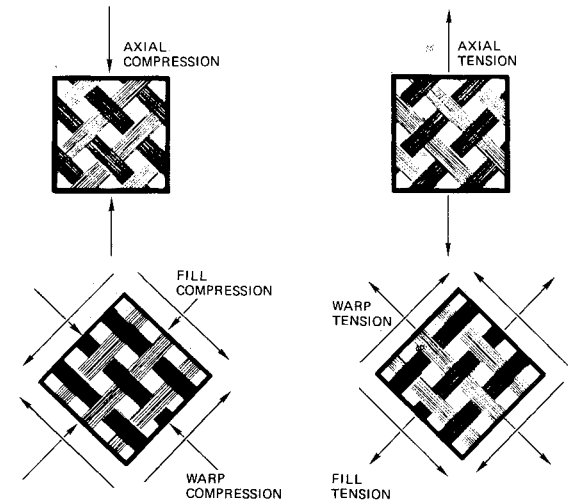

Fig. 12 Test cone 103 hoop strain comparisons.

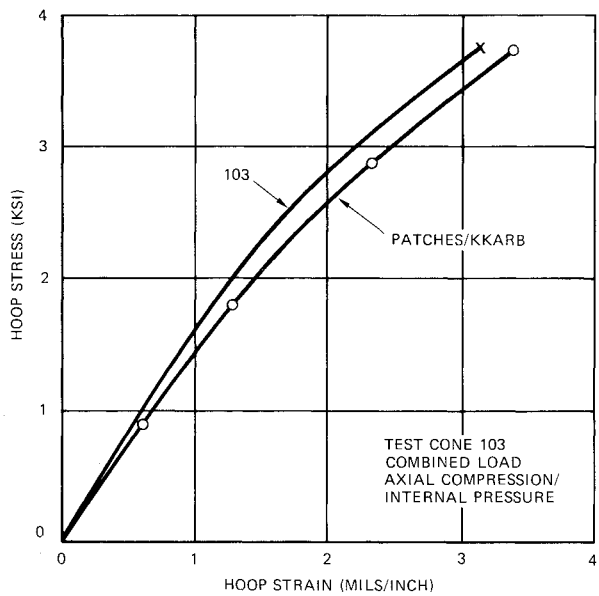

Fig. 13 Bimodular structural behavior.

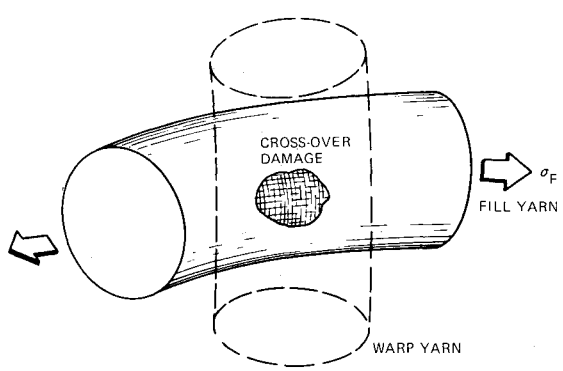

Fig. 14 Warp-fill crossover damage.

was −11,000 psi. These results indicate clearly that an involute cone can develop the full coupon compression strength of the material.

Test cone 102 was loaded by internal pressure to determine if nonlinear fill tension behavior observed in coupons and cylinders would describe the behavior of a cone. A plot of hoop stress-strain response, Fig. 10, shows good agreement between test and our analysis based on coupon data. A deformed geometry plot, Fig. 11, greatly magnified, shows meridional bending and transverse shear are present at the large diameter end where failure initiated.

Test cone 103 was the first combined load test of an involute cone under laboratory conditions. The axial load to internal pressure ratio of 100 to 1 was calculated to cause failure in the gage section and this is where fracture occurred. Interestingly, the pressure at failure was almost identical to cone 102, even though the cone was carrying −28,660 lb of axial load and failed at a completely different site. This cone failed very close to the load predicted before the test based on coupon strength and a polynomial failure surface.

Predicted hoop strains agreed reasonably well, Fig. 12, with the test data average value from gages 2, 4, and 5 at 0, 120, and 240 deg around the cone in the gage section. In this test, the hoop strain data had a much higher variation around the circumference than in any other test, even though the axial strain data from the very same points were uniform. These data also showed the cone slightly stiffer than predicted at every load level.

Conclusions and Recommendations

The bimodular nonlinear mechanical properties of 2D carbon-carbon materials have been characterized at room temperature and a new material model developed and validated in a finite element structural analysis program, PATCHES-III. The nonlinear mechanics of 2D carbon-

carbon proved to be very different than that of 3D or 4D carbon-carbons which tend to have all their nonlinearity associated with the matrix phase. A new deformation mechanism caused by warp-fill crossover damage is postulated that allows fill fiber tensile strains to reduce warp-fill shear stiffness. This accounts for bimodular structural behavior, Fig. 13, seen in earlier axial load tests of cylinders.[1] One important result was a demonstration that the nonlinear mechanics of 2D carbon-carbon determined from flat laminate specimens are also characteristic of that observed in composite cylinders and cones of involute construction.

This includes the strength of the material in that the full coupon strength of K-KARB was developed in combined load tests of involute cones. The statistical significance of these results and the possibility of scale effects are open questions. A need to better pin down the mechanics of crossover damage to determine what other properties might be affected and its morphology, Fig. 14, will require additional testing. Also, the effects of temperature on nonlinear properties need to be investigated. Room temperature testing did, however, demonstrate that initial tangent stiffness data only begin to describe the mechanics of 2D carbon-carbon composites.

In concluding this paper, it is appropriate to comment briefly on the distinction between the mechanics of an ideal material and a real material. It is particularly important for 2D carbon-carbon materials because of the variability in matrix-dominated properties. Exact analyses consisting of mathematical reasoning from universally valid laws are a myth for this class of composites. There is an inescapable ambiguity in an analysis of any particular structure associated with the as-built properties of the material in that structure. Under controlled conditions such as on this program, K-KARB behavior can be predicted with less than 10% difference between analysis and the average value of the composite strains, which is also typical of the variability in strains around the circumference of a cone. One approach to material modeling for this class of composites is to use multiple stress-strain diagrams for finite element computer analyses based on extensive characterization tests.

Acknowledgments

The authors wish to acknowlege the expert experimental work of Aerojet Strategic Propulsion Co. and the support of the Air Force Rocket Propulsion Laboratory under Contract F04611-80-C-0060 supervised by J. Hildreth. Portions of the work were also supported by PDA Corporate IRAD under Account No. 459200. The insight, counsel, and active participation of H. O. Davis and J. G. Crose also were essential to model development and are gratefully acknowledged.

References

[1]Davis, H. O. and Vronay, D. F., "Structural Assessment of Involutes," AFML-TR-79-4068, June 1979.

[2]Matthews, D. K. and Davis, H. O., "2D Material Response," AFRPL-TR-83-078, Vol. II, Nov. 1983.

[3]Jortner, J., "Modeling Nonlinear Stress-Strain Behavior of Carbon-Carbons with Wavy Yarns," Fifth Rocket Nozzle Technology Meeting (JANNAF RNTS), Colorado Springs, Colo., Dec. 1983.

[4]Barlow, J., "Optimal Stress Locations in Finite Element Models," *International Journal for Numerical Methods in Engineering*, Vol. 10, 1976, pp. 243-251.

[5]Pagano, N. J., "Elastic Response of Rosette Cylinders Under Axisymmetric Loading," *AIAA Journal*, Vol. 15, Feb. 1977, pp. 159-166.

[6]Hearle, J.W.S. et al., *Structural Mechanics of Fibers, Yarns, and Fabrics*, Vol. 1, Wiley-Interscience, 1969, Chap. 9.

[7]Jortner, J., "A Model for Predicting Thermal and Elastic Constants of Wrinkled Regions in Composite Materials," ASTM Symposium on Effects of Defects in Composite Materials, San Francisco, Calif., Dec. 1982.

[8]Jortner, J., "Multiaxial Response of ATJ-S Graphite," AFML-TR-73-170, Oct. 1973.

[9]Batdorf, S. B., "A Polyaxial Stress-Strain Law for ATJ-S Graphite," *Journal of the American Ceramic Society*, Vol. 59, 1976, pp. 308-312.

[10]Jones, R. M. and Nelson, D.A.R. Jr., "A New Material Model for Nonlinear Biaxial Behavior of ATJ-S Graphite," *Journal of Composite Materials*, Vol. 9, 1975, pp. 10-27.

[11]Owen, M. J., "Biaxial Failure of GRP-Mechanisms, Modes and Theories," *Composite Structures*, Vol. 2, Applied Science Publishers Ltd., 1983, pp. 21-39.

[12]Delneste, L. and Perez, B., "An Inelastic Finite Element Model of 4D Carbon-Carbon Composites," *AIAA Journal*, Vol. 21, Aug. 1983, pp. 1143-1149.

[13]Stanton, E. L., "A General Three-Dimensional Computational Model for Nonlinear Composite Structures and Materials," AIAA Paper 77-360, *Proceedings AIAA/ASME/SAE 18th SDM Conference*, 1977, pp. 9-22.

[14]Pagano, N. J., "General Relations for Exact and Inexact Involute Bodies of Revolution," *Advances in Aerospace Structures and Materials-AD-03,* edited by R. M. Laurenson and U. Yuceoglu, ASME, New York, 1982, pp. 129-137.

[15]Lin, T. H., *Theory of Inelastic Structures*, John Wiley & Sons, 1968, Chap. 2.

[16]Stanton, E. L. and Kipp, T. E., "A Model for Nonlinear 2D Carbon-Carbon Composite Materials and Structures," AIAA Paper 84-0956, *Proceedings AIAA/ASME/ASCE/AHS 25th SDM Conference*, 1984, pp. 322-332.